Mon. Not. R. astr. Soc. (1981) **196**, 597–610

Models of radio source evolution – II. The 2700-MHz source count

J. V. Wall★, T. J. Pearson† and M. S. Longair‡
Mullard Radio Astronomy Observatory, Cavendish Laboratory, Madingley Road, Cambridge CB3 0HE

Received 1981 January 9; in original form 1980 July 28

Summary. Our technique for deriving cosmological evolution from source counts and identifications is applied to data at 2700 MHz. The analysis is carried out on the assumption that two populations with different evolutionary behaviours appear in surveys at this frequency: 'steep-spectrum' sources with extended radio structures, and 'non-steep-spectrum' sources with compact structures, the majority of which are identified with QSOs. The 2700-MHz data add constraints to the evolution deduced for the 'steep-spectrum' sources from low-frequency data; in particular, of the two types of model obtained in our analysis of the 408-MHz data, only one now appears tenable. The present results for 'non-steep-spectrum' sources agree with the results from luminosity – volume tests on samples of 'flat-spectrum' QSOs – the change in space density with epoch appears less dramatic than for the powerful radio sources with steep spectra and extended radio structures.

1 Introduction

In Paper I (Wall, Pearson & Longair 1980) we described a self-consistent technique for deriving the cosmological evolution of extragalactic radio sources from source counts, identification and redshift data for the brighter sources. The scheme was applied to data at 408 MHz. In the present paper we employ the technique in a preliminary investigation of the cosmological implications of source counts and identifications at 2700 MHz.

Surveys at frequencies of 408 MHz and lower are dominated by 'steep-spectrum' (SS) sources with extended radio structures. As the survey frequency is raised, the proportion of 'centimetre-excess' or 'flat-spectrum' sources increases. The latter term is a misnomer, and is used to describe collectively the sources whose spectra are 'not steep', i.e. whose spectra are *not* power laws of spectral index $\alpha > 0.5$ ($S \propto \nu^{-\alpha}$) or power laws with such indices which bend to steeper power laws at higher frequencies. The so-called 'flat-spectrum' sources have

★ Present address: Royal Greenwich Observatory, Herstmonceux Castle, Hailsham, East Sussex BN27 1RP.
† Present address: Owens Valley Radio Observatory, California Institute of Technology, Pasadena, California 91125, USA.
‡ Present address: Royal Observatory, Blackford Hill, Edinburgh EH9 3HJ.

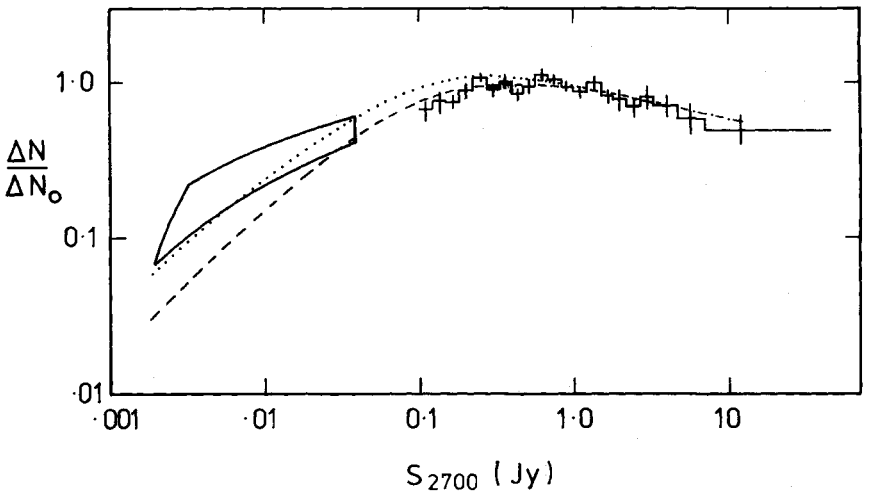

Figure 1. The total source count at 2700 MHz. In this relative differential form, ΔN is the number of sources with flux density between S and $S + \Delta S$, and ΔN_0 is the number computed from the 'Euclidean' law, i.e. $\Delta N_0 = 100\ [S^{-1.5} - (S + \Delta S)^{-1.5}]$. The error box at the faint flux densities represents the estimate of the source-count from $P(D)$ (background deflection) analysis. The smooth curves show total (model) counts formed by adding sub-counts computed for the 'steep-spectrum' (SS) sources and the 'non-steep-spectrum' (NSS) sources. Dotted curve: SS source evolution model 4b (parameters in the caption of Fig. 2) + NSS source evolution model of 'exponential' type with exponent $M = 7$. Dashed curve: SS evolution model 4b + NSS 'exponential' model with $M = 5$.

spectra which show flattening or inversion at the higher frequencies and/or cutoffs to the lower frequencies; the assortment of forms (which are anything but flat) is shown in Figs 2 to 12 of Wall (1972). To avoid the term 'flat-spectrum', we shall refer to these sources as 'non-steep-spectrum' (NSS). The structures of these sources are dominated by one or more compact components whose self-absorption gives rise to the cutoffs and inversions in the integrated spectra; some of the components are highly variable both in flux density and structure on time-scales as short as weeks. Most of the identified sources of this spectral type have QSOs as their optical counterparts (e.g. Peterson & Bolton 1973), and a few are identified with elliptical galaxies with active nuclei (e.g. Heeschen 1970; Kühr 1977).

The mapping of the cosmological evolution of NSS sources is essential in any attempt to understand the cosmic behaviour of radio sources in general, and this can be provided by systematic analyses of high-frequency source counts. There is some evidence that their radial distribution differs significantly from that of the powerful radio sources of the steep-spectrum type: V/V_{max} (luminosity–volume) analyses of samples of QSOs selected at high frequencies suggest a more uniform distribution (Schmidt 1976; Masson & Wall 1977). The consequences for general schemes of cosmological evolution (e.g. Grueff & Vigotti 1977) remain largely unexplored.

The frequency of 2700 MHz is optimum for a preliminary investigation. Some 60 per cent of the sources detected at this frequency are still of the SS variety, whose evolutionary properties should be comprehensible from our investigation of the 408-MHz data. The remaining 40 per cent of NSS sources constitute a large enough proportion to yield significant conclusions. There exists a well-defined source count, obtained from the Parkes survey at 2700 MHz (Fig. 1). Flux variability at this frequency is less than at higher frequencies, and does not give rise to serious epoch-dependence of the counts and complete samples. Moreover, accurate positions (± 2 arcsec) from the RRE-Malvern interferometer have yielded optical identifications for a sample which are based on positional coincidence alone (McEwan, Browne & Crowther 1975, hereafter MBC).

In the analysis of the 408-MHz count in Paper I, we assumed that all sources belonged to a single (SS) population. Here we assume that the counts at 2700 MHz consist of two populations, the SS and NSS sources. We allow the NSS sources to evolve independently of the SS population, and carry out the exploration of the 2700-MHz data separately for each.

2 The scheme at 2700 MHz

The extension of the scheme described in Paper I to two populations is straightforward. For each radio source population, we want to know $\rho(P, z)$, the radio luminosity function and its dependence on epoch. As in Paper I, the dependence of each population on epoch may be described explicitly with an evolution function F, i.e.

$$\rho(P, z) = F(P, z)\,\rho_0(P), \tag{1}$$

where ρ_0 is the local luminosity function $\rho(P, z = 0)$. For known F and ρ_0, the count may be computed from

$$N(>S) = \int_0^{\infty} dP \int_0^{z(S)} \rho_0(P) \cdot F(P, z) \cdot dV(z), \tag{2}$$

where $dV(z)$ is the volume element in the adopted geometry, and $z(S)$ is the redshift at which a source of power P has a flux density S, obtained from

$$S = P/D^2\,(1 + z)^{1+\alpha}. \tag{3}$$

The procedure for finding evolution functions consists of constructing a complete luminosity distribution $n(P)$ from the optical data for a sample of sources with $S \geqslant S_0$, and using this to obtain ρ_0 for each evolution function via

$$\rho_0(P)\,dP = n(P)\,dP \Big/ \int_0^{z(S_0)} F(P, z) \cdot dV(z). \tag{4}$$

The count computed via equation (2) can then be tested statistically against the observed count.

Thus the scheme requires (a) a luminosity distribution and (b) a source count, for each population at the frequency in question. To construct the two luminosity distributions for the SS and NSS populations, we adopted S_0 (2700 MHz) = 1.0 Jy; at this level the MBC sample yields 48 sources (Table 1) in 0.514 sr of the $\pm 4^\circ$ dec zone which is free of obscuration. Of these sources, 42 are identified, and 25 have redshift measurements. The sample provides luminosity distributions which suffer from serious statistical uncertainty, but a deeper sample from the zone cannot help because the proportion with redshift measurements falls rapidly with flux density. There is a great urgency for much larger complete samples of identified sources selected from high-frequency surveys; the sample of Peacock & Wall (1981), compiled after the present work was completed, goes some way to fulfilling this requirement. The classification of the sample of Table 1 into SS and NSS sources is straightforward because extensive spectral data are available (Wall 1972).

To obtain a source count for each of the two populations we proceeded as follows. Most sources from the Parkes 2700-MHz surveys have been observed at 5000 MHz, and high-frequency spectral indices α (2700–5000 MHz) are therefore available. Inspection of the spectra over the frequency range 178–5000 MHz (Wall 1972) indicates that, if α (2700– 5000 MHz) $\leqslant 0.5$, the source is invariably of the NSS type. The converse holds to a first approximation – a small proportion of NSS sources have α (2700–5000 MHz) > 0.5,

Table 1. A complete sample of sources with $S_{2700} \geqslant 1.0$ Jy.

(1) SOURCE PKS	(2) 3C	(3) S_{2700} Jy	(4) α_{HF}	(5) IDENT	(6) m_{pg}	(7) z	(8) log P_{2700}* W Hz^{-1} sr^{-1}	(9) Spectrum† SS	NSS
0003-00	2	2.41	0.77	QSO	21.4	1.037	27.02	✓	
0019-00		1.90	0.84	G	21.1	(0.48)	26.23	✓	
0034-01	15	2.56	0.75	EO	17.6	0.0733	24.68	✓	
0035-02	17	4.04	0.68	E	19.6	0.2201	25.84	✓	
0036+03		1.10	0.84	E2	14.5	0.0145	22.90	✓	
0051-03	26	1.11	1.03	EO	18.9	0.2106	25.27	✓	
0055-01	29	3.46	0.56	EO	15.9	0.0450	24.38	✓	
0056-00		1.80	0.47	QSO	17.6	0.717	26.48		✓
0106+01		1.88	-0.67	QSO	19.1	2.099	26.84		✓
0112-017		1.38	-0.23	QSO	18.4	1.366	26.65		✓
0122-00		1.43	0.25	QSO	17.0	1.070	26.66		✓
0123-01	40	2.75	0.91	db	13.7	0.0180	23.49	✓	
0137+012		1.07	0.48	QSO	17.0	0.262	25.40		✓
0218-02	63	1.68	1.14	E	20.6	(0.37)	25.98	✓	
0240-00	71	3.12	0.76	Sey	9.7	0.00344	22.10	✓	
0305+03	78	5.33	0.54	D	15.3	0.0289	24.18	✓	
0325+02	88	3.18	0.70	D	15.7	0.0302	24.00	✓	
0421+00		1.00	0.84	-	-	(0.5)	25.99	✓	
0422+00		1.29	-0.32	BSO	16.6	(1.0)	26.38		✓
0431-02		1.06	0.91	G	21.1	(0.48)	25.98	✓	
0440-00		3.53	0.08	QSO	19.1	0.848	26.82		✓
0457+024		1.63	0.18	QSO	19.3	2.383	27.29		✓
0458-02		1.99	0.16	QSO	19.6	2.286	27.34		✓
0723-008		3.01	0.21	NSO	18.4	(1.5)	27.23		✓
0724-01	180	1.56	0.92	G	20.0	(0.28)	25.66	✓	
0736+01		2.42	0.09	QSO	17.7	0.191	25.45		✓
0743-006		1.40	-0.43	NSO	17.6	(1.5)	26.64		✓
0812+02		1.18	0.69	QSO	17.6	0.402	25.84	✓	
0906+01		1.20	0.23	QSO	17.6	1.021	26.54		✓
0949+00	230	1.53	1.35	-	-	(0.5)	26.26	✓	
1039+02		1.66	0.82	-	-	(0.5)	26.20	✓	
1055+01		3.02	0.00	QSO	18.7	0.888	26.76		✓
1059-01	249	1.34	1.10	-	-	(0.5)	26.16	✓	
1138+01		1.57	0.72	-	-	(0.5)	26.16	✓	
1148-00		2.56	0.39	QSO	17.6	1.982	27.45		✓
1215+03		1.21	1.33	E,D	18.0	0.076	24.40	✓	
1226+02	273	43.4	0.04	QSO	13.0	0.158	26.54		✓
1229-02		1.33	0.45	QSO	17.1	1.043	26.66		✓
1330+02	287.1	1.91	0.50	N	18.9	0.2156	25.48	✓	
2044-02		1.38	0.60	G	20.5	(0.35)	25.77	✓	
2131-021		1.91	-0.15	QSO	19.1	0.557	26.18		✓
2134+004		7.59	-1.02	QSO	17.7	1.935	27.25		✓
2210+01		1.79	0.79	-	-	(0.5)	26.23	✓	
2216-03		1.04	-0.30	QSO	16.2	0.901	26.23		✓
2221-02	445	3.46	0.81	N	17.3	0.0568	24.59	✓	
2313+03	459	2.38	0.94	N	18.2	0.2205	25.63	✓	
2324-02		1.56	0.75	EO	18.9	(0.17)	25.20	✓	
2349-01		1.01	0.74	N	17.1	0.174	25.04	✓	

*H_0 = 50 km s^{-1} Mpc^{-1}; Ω = 1.0.

†SS ≡ 'steep-spectrum'; NSS ≡ 'not-steep-spectrum', or 'flat-spectrum'.

namely those with single spectral peaks in the frequency range 200–2000 MHz. Ignoring this detail, we constructed the separate counts for SS and NSS sources, using the sources from the survey for which α(2700–5000 MHz) exists, and adopting the criterion that the source is classified as SS if $\alpha > 0.5$ and NSS if $\alpha \leqslant 0.5$. The two counts (Table 2) were constructed from the zones of the survey with differing completeness limits at 2700 MHz, the total area being much smaller for the fainter sources. Bolton, Savage & Wright (1979) give references for the 15 parts of the survey now completed.

The faint end of the total count (Fig. 1) is defined by statistical ($P(D)$) methods (Wall &

Table 2. The 2700-MHz source counts.

S_{2700} (Jy)	All sources ΔN	Area (sr)	$\Delta N/\Delta N_o$	('flat-spectrum') NSS $\Delta N/\Delta N_o$	('steep-spectrum') SS $\Delta N/\Delta N_o$
∞	19	6.94	0.494	$.156^{.220}_{.111}$	$.338^{.432}_{.265}$
6.8	17	6.94	0.588	$.207^{.292}_{.147}$	$.380^{.494}_{.292}$
4.7	34	6.94	0.716	$.211^{.278}_{.160}$	$.505^{.608}_{.419}$
3.3	33	6.94	0.814	$.394^{.492}_{.315}$	$.419^{.522}_{.337}$
2.7	39	6.94	0.697	$.179^{.235}_{.136}$	$.518^{.614}_{.437}$
2.2	59	6.94	0.794	$.323^{.389}_{.268}$	$.471^{.551}_{.403}$
1.8	74	6.94	0.825	$.245^{.297}_{.202}$	$.579^{.656}_{.511}$
1.5	149	6.94	1.001	$.342^{.339}_{.300}$	$.658^{.724}_{.598}$
1.2	146	6.94	0.889	$.299^{.342}_{.262}$	$.590^{.650}_{.536}$
1.0	224	6.94	0.943	$.240^{.272}_{.212}$	$.703^{.757}_{.652}$
0.82	317	6.94	1.063	$.319^{.352}_{.289}$	$.745^{.795}_{.698}$
0.68	140	2.11	1.123	$.234^{.275}_{.195}$	$.827^{.905}_{.756}$
0.56	140	2.11	0.948	$.269^{.310}_{.233}$	$.789^{.859}_{.724}$
0.47	173	2.11	0.842	$.367^{.414}_{.326}$	$.881^{.953}_{.814}$
0.39	160	1.383	1.024	$.232^{.269}_{.199}$	$.721^{.787}_{.655}$
0.33	190	1.180	0.906	$.279^{.319}_{.239}$	$.627^{.684}_{.570}$
0.27	254	0.966	1.080	$.303^{.356}_{.250}$	$.776^{.846}_{.706}$
0.22	105	0.372	0.883	$.274^{.334}_{.214}$	$.609^{.689}_{.529}$
0.18	23	0.0753	0.747	$.205^{.306}_{.137}$	$.543^{.696}_{.424}$
0.15	39	0.0753	0.764		
0.12	39	0.0753	0.692	$.127^{.195}_{.083}$	$.598^{.693}_{.516}$
0.10					

Notes to Table 2

(1) Counts made from the first 10 parts of the Parkes 2700-MHz survey (see Bolton, Savage & Wright 1979 for references)

(2) ΔN_o calculated from $N_o = 100\ S_{2700}^{-1.5}$

(3) Errors on $(\Delta N/\Delta N_o)$ for total count are given by $(1/\Delta N)^{\frac{1}{2}}$

(4) At flux densities above the horizontal line, all catalogued sources from which the counts were constructed have flux density measurements at 5000 MHz, and hence could be classed as 'steep-spectrum' or 'non-steep-spectrum' (SS or NSS; see text). For fainter flux densities, incomplete 5000-MHz flux-density measurements were used to estimate proportions of the total count ΔN which are SS or NSS, and the errors on $(\Delta N/\Delta N_o)$ include uncertainties in estimating this proportion. The 5000-MHz flux densities used in estimating the proportions at $0.18 > S_{2700} > 0.10$ Jy are from Savage (1978) and Wall, A.E. Wright, A. Savage & J.G. Bolton (in preparation).

Cooke 1975 and unpublished data), and for this region, separation of the count into SS and NSS components is not possible. However, some information on spatial distribution may be derived, because the *sum* of counts computed for the SS and the NSS populations must agree with it (Section 5).

Throughout we adopt the Einstein–de Sitter geometry ($\Omega = 1$, $\Lambda = 0$) and a Hubble constant of 50 km s^{-1} Mpc^{-1}.

3 The 'steep-spectrum' (SS) component at 2700 MHz

It might be argued that the SS component at 2700 MHz can add nothing to the results from the 408-MHz investigation. Such is not the case, because samples of SS sources selected at 2700 MHz are not identical to those selected by 408-MHz surveys (Condon & Jauncey 1974). The change comes about via the P–α correlation (e.g. Kellermann, Pauliny-Toth & Williams 1969; Véron, Véron & Witzel 1972); the SS sources selected at high frequencies have statistically flatter spectra than those found at low frequencies, thus biassing the samples to lower luminosities. The difference is significant but not drastic, and the sets of complete samples of SS sources at 408 and 2700 MHz have a large intersection. In the present work, limited as it is by the poor statistics of the luminosity distribution, we test whether the two successful models of evolution found in Paper I (models 4 and 5) meet with similar success in describing the SS source data at 2700 MHz.

3.1 SOURCE COUNT AND LUMINOSITY DISTRIBUTION OF THE SS SOURCES

The count for SS sources (Table 2) is shown in Fig. 2. The initial rise is somewhat steeper than that of the total count (Fig. 1), and the general form resembles that of the 408-MHz count (Fig. 2 of Paper I).

The luminosity distribution for the SS sources is shown in Fig. 3. It consists of 16 galaxies with measured redshifts, six galaxies with redshifts estimated from the m–z relation as described in Paper I, two QSOs with measured redshifts, and six unidentified sources for which we estimated redshifts (as in Paper I) by assuming that the optical counterparts are

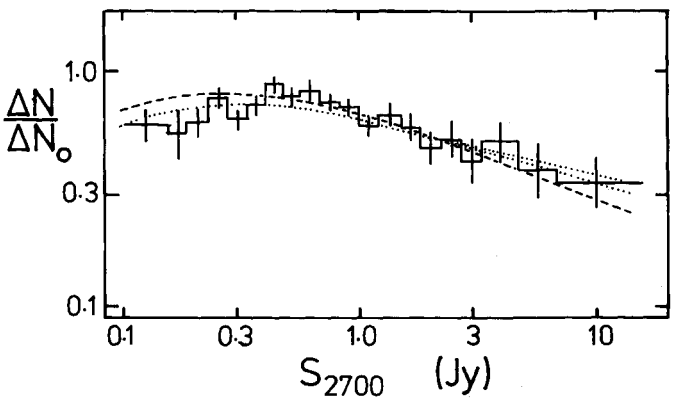

Figure 2. The relative differential source count for 'steep-spectrum' (SS) sources. The smooth curves represent counts computed for different evolution models as described in the text. Dotted curves: SS model 4 (from Paper I), for which $F(P, z) = \exp[M(P)(1 - t/t_0)]$, $M(P) = 0$ for $P < P_1$, $M_{\max}(\log P - \log P_1)/(\log P_2 - \log P_1)$ for $P_1 < P < P_2$, and $M_{\max}$ for $P > P_2$. The upper dotted curve is model 4a for which parameters at 2700 MHz are $z_c = \infty$ (i.e. no redshift cutoff), $\log(P_1/\mathrm{W\,Hz^{-1}\,sr^{-1}}) = 25.4$, $\log P_2 = 26.5$ and $M_{\max} = 11.5$. The lower dotted curve is for model 4b, $z_c = 3.5$, $\log P_1 = 24.4$, $\log P_2 = 26.7$. Dashed curve: model 5 for which $F(P, z) = \chi_1(P) + \phi\chi_2(P)$, where $\phi = \exp[M(1 - t/t_0)]$, $\chi_1 = (P_t/P)^m/[1 + (P_t/P)]^m$, $\chi_2 = 1/[1 + (P_t/P)^m]$, and $\log P_t = a \log z + b$. Parameters at 2700 MHz are $M = 9.8$, $a = 3.14$, $b = 26.2$, $m = 1.06$.

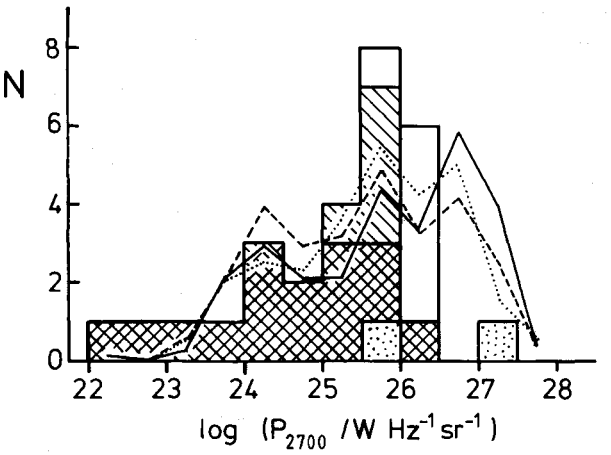

Figure 3. The luminosity distribution, $S_{2700} \geqslant 1.0$ Jy, for SS sources in the ± 4° declination zone of the Parkes 2700-MHz survey. Cross-hatched areas: galaxy identifications with redshift measurements; singly-hatched areas: galaxy identifications with redshift estimates; dotted areas: QSO identifications with redshift measurements; blank areas: unidentified sources for which redshifts were estimated on the assumption that the optical counterparts are galaxies just beyond the limiting magnitude of the Palomar Sky Survey. The lines represent predictions of this distribution from the 408-MHz data, using evolution functions (see caption, Fig. 2) and spectral indices as described in Section 3.1. The solid line is the distribution calculated from model 4b while the dashed line is that from model 5. The dotted line is the distribution calculated from model 5 with all spectral indices set to $\alpha(408\text{–}2700\,\text{MHz}) = 0.75$; it demonstrated that the P–α correlation does not have a major effect on the form of the luminosity distribution at 2700 MHz.

galaxies just fainter than the limit of the Palomar Survey prints. All identification, magnitude and redshift data are from MBC and references therein.

The distribution contains a mere 28 sources, of which only 16 (57 per cent) have measured redshifts. It is possible to test whether this limited sample and the redshift estimates have produced a representative luminosity distribution for SS sources at 2.7 GHz. A large, complete and fully identified sample of SS sources, selected at a frequency of ν_1 may be used to predict the luminosity distribution at ν_2 provided that the evolution function is known. If the sample at ν_1 is complete to S_1, then each source contributes to the ν_2 luminosity distribution

$$n(P_2, S_2) = \int_0^{z_2} F(P_1, z) \cdot dV(z) \Big/ \int_0^{z_1} F(P_1, z) \cdot dV(z) \qquad (5)$$

sources of luminosity $P_2 = P_1(\nu_1/\nu_2)^\alpha$, where α is the two-point spectral index between frequencies ν_1 and ν_2, F is the evolution function, S_2 is the flux density at which the luminosity distribution at ν_2 is to be predicted, and z_1 and z_2 are solutions of (3) for (P_1, S_1, α) and (P_2, S_2, α) respectively. This calculation builds in the P–α correlation automatically, because each source in the original sample has its own value of α.

To predict a 2700-MHz luminosity distribution for the SS sources, we used 84 sources from the 87-source sample which defined the 408-MHz luminosity distribution (Fig. 3 of Paper I), rejecting from it the three NSS sources (3C 273, 286 and 454.3). We obtained each $\alpha(408\text{–}2700\,\text{MHz})$, and for each source calculated its contribution to a luminosity distribution for $S_{2700} \geqslant 1.0$ Jy via equation (5). The prediction was carried out for each of the successful evolution models of Paper I, and the resulting distributions are shown in Fig. 3. These are not in particularly good agreement with the luminosity distribution of the 28-source sample; the predicted distribution from model 5 differs at the 15 per cent level of confidence, while those from models 4a and 4b differ at a level of confidence below 0.01 per cent. (The effect of the P–α correlation is relatively minor; if all α are set as 0.75, the

resulting distributions are in slightly poorer agreement as shown.) It is possible to produce better agreement – and in fact acceptable statistical agreement – if some of the unidentified sources are assigned higher redshifts. This *a posteriori* process is hard to justify, and it is more straightforward to adopt the predicted luminosity distributions in evaluating the evolution of SS sources from the 2700-MHz source count, noting that the technique can no longer be described as 'self-consistent' because we are using an SS luminosity distribution which differs from that given by the sample of Table 1.

3.2 EVOLUTION OF THE SS SOURCES

For each of the successful evolution models of Paper I, we calculated the SS count at 2700 MHz via equations (2) and (4). In the process we used the computed luminosity distribution appropriate to each model, and we normalized the counts to yield the same (integral) surface density at $S_{2700} = 1.0$ Jy as that of the observed SS count, namely 54.1 source sr^{-1}. This normalizing procedure is essential to remove the statistical uncertainty otherwise imposed on the vertical scaling by the limited number of sources in the luminosity distribution. The calculated counts are shown in Fig. 2, superposed on the observed SS count.

The different models predict counts which are quite distinct. The two dotted curves refer to the two versions of the first of the successful models i.e. 4a and 4b, the former having no redshift cutoff, the latter a cutoff at $z = 3.5$. These curves follow the observed SS count well, except within the region $0.4 < S_{2700} < 0.9$ Jy where they fall below the data. A χ^2 test indicates that overall disagreement between these curves and the observations could arise by chance nine times out of 100; considering its success in describing the 408-MHz data, the model may be said to survive the present SS data.

The same cannot be said of the other model (model 5, again described in the legend of Fig. 2). It provides an excellent fit for $S_{2700} > 0.4$ Jy, but at lower flux densities the fit is very poor. The calculated count does not turn over rapidly enough and in fact it predicts that *all* sources detected at $S_{2700} < 0.2$ Jy must be of the SS type. This is not true; some 25 per cent of sources in the range $0.1 < S_{2700} < 0.2$ are observed to have α(2700–5000 MHz)< 0.5. The extended region of turnover for this model arises because it ascribes considerably more evolution to low-power sources than does the previous model. The 'excess' at faint intensities occurs because the evolving component is considerably broadened as a result, and the region of turnover will be correspondingly wider. It was suggested in Paper I that model 5 predicted proportions of identifications in excess of those observed at the fainter 408-MHz flux densities. The present work provides further indication that the model is untenable, and the different sample of SS sources selected at 2700 MHz has thus set further constraints on permissible forms of the evolution function $F(P, z)$ for SS sources.

4 The 'non-steep-spectrum' (NSS) component at 2700 MHz

The SS source analyses of Paper I and Section 3 provide no guidelines in that the NSS sources differ drastically in morphology from the SS sources, having structures on scales of pc or tens of pc rather than kpc; there is no physical reason why their radial distribution should bear any resemblance either.

4.1 SOURCE COUNT AND LUMINOSITY DISTRIBUTION OF THE NSS SOURCES

The NSS source count (Table 2) is shown in Fig. 4. It shows an extended 'Euclidean' region, and this relatively flat count for NSS sources provides the change observed in the form of total source counts as survey frequency is raised and the detection rate of NSS sources increased (see, e.g. Fig. 1 of Wall 1980).

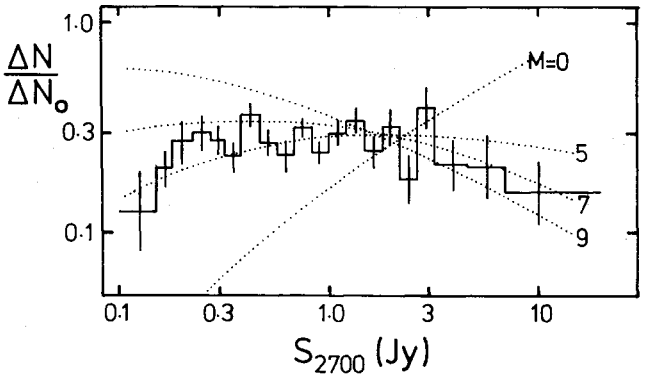

Figure 4. The relative differential source count for 'non-steep-spectrum' (NSS) sources. The smooth curves represent counts computed for the simple 'exponential' evolution model $F(P, z) = F(z) = \exp [M(1 - t/t_0)]$ for various values of M as shown; $M = 0$ represents a uniform distribution.

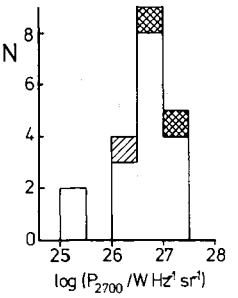

Figure 5. The luminosity distribution, $S_{2700} \geqslant 1.0$ Jy, for NSS sources in the ± 4° declination zone of the Parkes 2700-MHz survey. Blank areas: QSOs with measured redshifts; cross-hatched areas: QSOs of 'neutral' colours with guessed redshifts; hatched area: QSO with guessed redshift.

The NSS luminosity distribution (Table 1) is shown in Fig. 5. It comprises 17 QSOs with measured redshifts, one blue stellar object, and two stellar objects of 'neutral' colour. The latter three objects are probably QSOs, and to 'complete' our luminosity distribution we assigned redshifts of 1.0 to all of them. The total sample (20) is too small to provide a luminosity distribution whose features are accurately defined; however, unlike the SS distribution, redshifts for most of the objects (17/20 or 85 per cent) are known. The sample contains no 'active' galaxies. Complete samples of NSS sources over larger areas of sky do so (e.g. Kühr 1977; Peacock & Wall 1981), and there are famous objects of this type, e.g. 3C 84, NGC 1052. For the present, the fact that no such objects appear in Fig. 5 suggests that the assumption that all NSS objects belong to a single population, namely QSOs with compact radio structure, is a reasonable first approximation.

4.2 EVOLUTION OF THE NSS SOURCES

The approximately Euclidean behaviour of the NSS source count over a large flux density range (Fig. 4) has led some observers to suggest that these objects have a uniform spatial distribution. However, the radio sources involved have high luminosities and consequently lie at redshifts where the 'corrections' to the Euclidean predictions are large in Friedmann world models. A calculation of the count anticipated for uniform spatial distribution in a Friedmann Universe, $\Omega = 1$, yields the curve shown in Fig. 4. This curve (computed for the luminosity distribution of Fig. 5 and from equations (2) and (4) in accordance with the scheme of Section 2) bears no resemblance to the observed count. Indeed, the cosmological redshifts of the objects must all be < 0.1 in order to obtain a count for uniform radial distribution which agrees with the observed NSS count.

The limitations of the data preclude the kind of search for evolution models of Paper I. Because the observed luminosity distribution is relatively narrow, in this preliminary analysis we ascribe the same evolution to all luminosities of NSS sources, unlike the SS sources for which the broad luminosity distribution means that differential evolution between high- and low-power sources is essential. We adopt simple density evolution

$$F(P, z) = F(z) = \exp\,[M(t_0 - t)/t_0] \tag{6}$$

with no redshift cutoff, where t_0 is the present epoch and t the epoch at which the source emitted the radiation, and ask what values of the single parameter M provide satisfactory descriptions of the count data.

The most luminous SS sources require values of $M > 9$ to fit the data (Paper I). For this exponent, the count computed via the technique of Section 2 is shown in Fig. 4; the overall fit to the count data is almost as bad as for the uniform model ($M = 0$). Values of M between 5 and 7, however, produce reasonable representations of the NSS count as shown. Such moderate evolution is in agreement with results from the luminosity–volume ($V/V_{\max}$) test for NSS QSOs. For the $M = 5$ case, calculation of $\langle V/V_{\max} \rangle$ for the radio-limited objects yields a value of 0.62 at $S_{2700} = 0.35$ Jy; values of 0.56 to 0.64 have been obtained for samples of NSS QSOs (Schmidt 1976; Masson & Wall 1977; Wills & Lynds 1978). Although the value of 0.62 is a lower limit, the true value of $\langle V/V_{\max} \rangle$ cannot be much higher, because for most of these objects it is the radio limit which defines the values of $V/V_{\max}$, as can be demonstrated directly for the 20-source sample.

Our analysis thus shows that the relatively flat source counts at the higher frequencies and the lower values found for $V/V_{\max}$ for samples of NSS QSOs are manifestations of the same thing – the relatively mild cosmic evolution of these objects, an increase in space density with lookback time which appears to be less than that of the SS sources of the same radio luminosity. Source-count analysis and $V/V_{\max}$ data thus yield quantitatively similar results for this evolution, as indeed they must for any class of object (Longair & Scheuer 1970). It is probable, though, that to ascribe 'milder cosmic evolution' to all NSS sources is an oversimplification. Fig. 4 shows that single-parameter evolution does not provide a good fit for the NSS count; there is a steep initial portion with a slope close to that of the $M = 9$ curve, while the diminution at fainter flux densities follows curves for $M \leqslant 5$. This suggests that differential evolution may be present in the same sense as for the SS sources, the more luminous NSS sources evolving rapidly while the less luminous sources show little or no change in space density with epoch. The present data are not adequate to explore this, but they do show that quantitatively the luminosity function of NSS sources and its cosmic evolution must differ from those of the SS sources.

4.3 THE LOCAL LUMINOSITY FUNCTION OF NSS SOURCES

The local luminosity function corresponding to an evolution function $F(z) = \exp\,[5\,(t_0 - t)/t_0]$ is shown as the heavy line in Fig. 6. The three-sectional appearance results from using a binned luminosity distribution; the numbers were too small to use the distribution in an unbinned-smoothed form as we did for the 408-MHz analysis (Paper I, Fig. 3).

Despite this, agreement with other estimates of the local space density for NSS sources is good. In particular, the function derived by Fanti *et al.* (1975) for 'flat-spectrum' QSOs from the B2 catalogue closely follows the present estimate. Fig. 6 also shows the radio luminosity function at $z = 1.0$ obtained by Wills & Lynds (1978) from a $V/V_{\max}$ analysis for a complete sample of NSS QSOs. When our local luminosity function is 'evolved' back to this redshift, the resulting space densities are lower than those of Wills & Lynds, but in view of the small numbers of sources involved and the uncertainty in the parameter M, this difference cannot be considered serious. The comparison cannot be precise in any case, because the

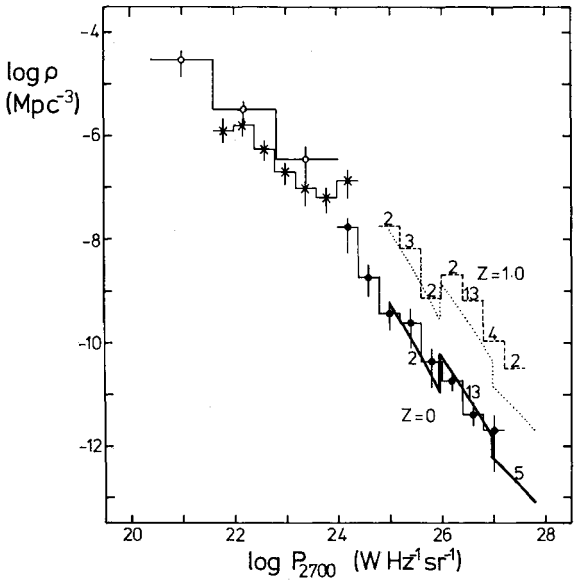

Figure 6. The local luminosity function for 'flat-spectrum' NSS QSOs. The heavy line corresponds to the present estimate, and the numbers against each section represent the numbers in the bins of the luminosity distribution (Fig. 5) used in its derivation. Open circles represent the (local) space densities for flat-spectrum nuclei found by Ekers & Ekers (1973) in their survey of E galaxies, while crosses represent the radio luminosity function obtained for the cores of E galaxies by Colla *et al.* (1975). Filled circles represent the local luminosity function for 'flat-spectrum' QSOs determined from sources of the B2 catalogue (Fanti *et al.* 1975). The dashed steps show the luminosity function determined for $z = 1.0$ by Wills & Lynds (1978) from a sample of NSS QSOs from the Parkes 2700-MHz survey; the numbers sitting on each step are the numbers of QSOs from which the step was derived. The dotted curve represents the present local luminosity function 'evolved' to epoch $z = 1.0$ using $F(z) = \exp[5(1 - t/t_0)]$.

present calculations are in the $\Omega = 1$ geometry, while those of Fanti *et al.* and of Wills & Lynds use $\Omega = 2$. The continuity between the local space densities for compact NSS QSOs and for cores of active galaxies has been noted previously (e.g. Fanti *et al.* 1975).

5 The total count

We have thus found two satisfactory models for the SS sources (models 4a and 4b of Paper I), and two models ('exponential', exponent $M = 5$ and $M = 7$) which approximately describe the evolution permissible for NSS sources. Further constraints can be obtained by adding these sub-counts and comparing the *total* predicted 2700-MHz count with the total observed count.

Results are shown in Fig. 1. The two successful models for SS sources (4a and 4b) provide sub-counts which are very similar, and hence we consider only one of them, namely that for model 4b, the model with a redshift cutoff $z_c = 3.5$. Adding each of the two sub-counts ($M = 5$ and $M = 7$) for the NSS sources to this curve yields the two total counts shown by smooth curves in Fig. 1. The total count for the $M = 7$ model overestimates surface densities in the region $0.1 < S_{2700} < 0.4$ Jy. However, it does pass through the error box provided by the $P(D)$ analysis defining the count at faint flux densities. On the other hand, the total count with $M = 5$ results in a curve which represents the total direct count very well, but which passes below the $P(D)$ error box. In fact, this is the lesser of the two evils: the $P(D)$ error box is not a good way of representing the results of background-deflection analysis. In this analysis, the count in the region of interest is assumed to be power-law in form, i.e.

$$dN = K S^{-\gamma} dS, \tag{7}$$

and for each value of γ, upper and lower limits to K are derived. The curved box crudely represents the $\pm 1\sigma$ range for a set of such laws corresponding to permissible values of γ.

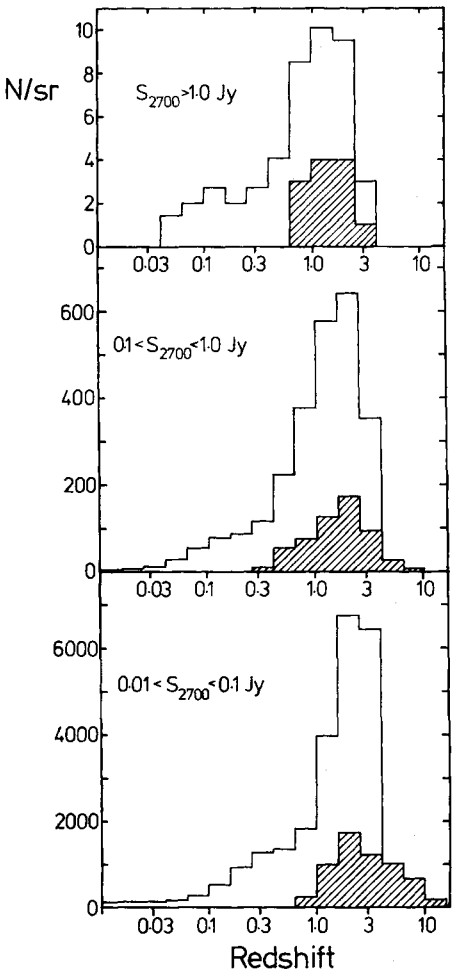

Figure 7. Histograms of the redshift distributions predicted by evolution model 4b for the SS sources, + 'exponential' model, $M = 5$, for the NSS sources. The SS sources are represented by the blank areas, while hatched areas correspond to the NSS sources. The effect of the redshift cutoff in model 4b ($z = 3.5$) for the SS sources is evident.

The $P(D)$ data are best suited to testing individual (predicted) models of the source count, and in future analyses of evolution models – analyses on more secure statistical bases than the present – it will be advisable to follow such a procedure.

Fig. 7 shows the distributions of redshifts at different flux densities for a total count composed of SS sources evolving according to model 4b and NSS sources following exponential evolution with $M = 5$. As well as the total redshift distribution, the histograms indicate the numbers of sources per sr of each type for each of the three flux-density bins. For the NSS sources, a slow progression to higher redshifts with decreasing flux density is apparent. For the SS sources, this progression is necessarily halted by the redshift cutoff at $z_c = 3.5$, and this in turn results in a narrowing of the distribution in luminosity.

6 Discussion and conclusions

The combination of models in Fig. 7 is illustrative only, and more complex models could be obtained to provide a greatly improved fit to the total count. This process has not been pursued, primarily because the inadequacy of the data for luminosity distributions, Table 1, has seriously limited the present investigation. For instance, the solution for the SS sources is not self-consistent in the sense of Paper I: the luminosity distribution is calculated, and does not agree well with that compiled for the $\pm 4^\circ$ declination zone. The lack of self-consistency

is evident in Fig. 7, which shows a significantly larger proportion of SS sources at redshifts > 0.5 than does the compiled distribution of Fig. 3. The computed SS-source luminosity distributions at 2700 MHz are in excellent agreement with preliminary versions of luminosity distributions compiled at $S_{2700} = 1.5$ Jy over ~ 4 sr (Peacock & Wall 1981). The discrepancy with the histogram of luminosities compiled here is due either to erroneous estimates of redshifts in Table 1, or to the fact that the sample of sources in the $\pm 4^\circ$ declination zone is not representative of samples over larger areas. With regard to the NSS sources, the luminosity distribution (Fig. 5) again is poorly defined; the sample is too small, although most members do have measured redshifts. Unlike the SS sources, complete and statistically adequate samples of NSS sources do not exist at other frequencies from which to compute the 2700-MHz distribution. A preliminary version of the NSS source luminosity distribution obtained by Peacock & Wall (1981) is in statistical agreement with Fig. 5. Nevertheless, the data of Fig. 5 are an inadequate basis on which to explore differential evolution of the NSS sources, although the data suggest that it is present.

There have been previous attempts to relate source-count, spectral-index and identification data at different frequencies. To do so, Fanaroff & Longair (1973) assumed a generalized luminosity function of the form

$$\rho(P, z, \text{spectrum}) = \eta(\alpha) \cdot \rho_0(P) \cdot F(P, z), \tag{8}$$

where $\eta(\alpha)$ is the spectral-index function. The formulation can only be valid for one particular frequency; Fanaroff & Longair demonstrated that it works (i.e. $\eta(\alpha)$ is independent of radio luminosity) to a first approximation at 178 MHz. With this and the evolution models of Doroshkevich, Longair & Zeldovich (1970), Fanaroff & Longair predicted source counts and spectral index distributions as a function of flux density at 5000 MHz. Agreement with survey and spectral data available at the time was very encouraging. Subsequent observations, however, have shown that the 5000-MHz counts do not fall off to the fainter flux densities as rapidly as the models suggested (Pauliny-Toth 1977). But of greater importance has been the indication from complete samples of NSS QSOs (Schmidt 1976; Masson & Wall 1977) that such objects appear to be more uniformly distributed in space than the SS sources. The Fanaroff–Longair models explicitly assumed that both SS and NSS sources could be described by a single luminosity function $\rho = \rho_0 F$, where the change with epoch dependence is given by a universal evolution function F. For this same reason, Schmidt's (1972) description of evolution is inadequate.

Kulkarni (1978) overcame this shortcoming by adopting different evolutions for 'flat' and 'steep' spectrum sources, together with different (Gaussian) spectral-index distributions for each population. Further, he introduced the P–α correlation in a parametric form. His calculations predicted source counts at 408 and 5000 MHz, together with distributions of spectral indices at various flux-density levels, which are in good agreement with most of the current data. However, Kulkarni assumed that the local luminosity function derived in Paper I encompassed both flat- and steep-spectrum sources. This function was derived from the 408-MHz data alone, and in fact describes only the steep-spectrum sources. Furthermore, Kulkarni's approach results in a very large set of parameters. He gives little indication of which are the critical ones, of permissible ranges for any of the parameters, or of how he obtained the single successful set which he presents.

Our approach is simpler; it represents the first attempt to analyse a high-frequency count directly. We assume that only two populations of extragalactic sources are present in surveys at frequencies of 2700 MHz and below, namely 'steep-spectrum' (SS) sources with extended structures and of the type which dominate low-frequency catalogues, and 'flat-spectrum' (or better, 'non-steep-spectrum', NSS) sources, whose proportion increases as survey fre-

quency is raised. The analysis does not describe the precise distribution of spectral indices at different flux-density levels. However, the important point is the technique of dividing total count into SS and NSS subcounts (and their separate fitting), which ensures that successful models for SS and NSS source evolution produce proportions of these at each flux density level in agreement with observation.

The present analysis is preliminary because of the inadequacy of the data; the main result is to clarify where observational effort is needed. It is evident that large and complete samples of identifications at frequencies $\geqslant 2700$ MHz are of paramount importance, in order to define luminosity distributions – particularly for the NSS sources. A requirement of lesser importance is the improved definition of source spectra and structure so that SS and NSS sources can be distinguished with confidence. Finally, there remains the need to improve the definition of the counts (and sub-counts if possible) at mJy levels for the higher frequencies.

Acknowledgments

JVW thanks the Royal Society for support via a Jaffé Donation Research Fellowship. TJP thanks the SRC for a Research Studentship held during early stages of the investigation, and the US NSF for partial support during the later stages. We are very grateful to the referee for a number of helpful comments.

References

Bolton, J. G., Savage, A. & Wright, A. E., 1979. *Aust. J. Phys. Astrophys. Suppl.*, **46**, 1.
Colla, G., Fanti, C., Fanti, R., Gioia, I., Lari, C., Lequeux, J., Lucas, R. & Ulrich, M.-H. 1975. *Astr. Astrophys.*, **38**, 209.
Condon, J. J. & Jauncey, D. L., 1974. *Astr. J.*, **79**, 437.
Doroshkevich, A. G., Longair, M. S. & Zeldovich, Ya. B., 1970. *Mon. Not. R. astr. Soc.*, **147**, 139.
Ekers, R. D. & Ekers, J. A., 1973. *Astr. Astrophys.*, **24**, 247.
Fanaroff, B. L. & Longair, M. S., 1973. *Mon. Not. R. astr. Soc.*, **161**, 393.
Fanti, C., Fanti, R., Ficarra, A., Formiggini, L., Giovannini, G., Lari, C. & Padrielli, L., 1975. *Astr. Astrophys.*, **42**, 365.
Grueff, G. & Vigotti, M., 1977. *Astr. Astrophys.*, **54**, 475.
Heeschen, D. S., 1970. *Astrophys. Lett.*, **6**, 49.
Kellermann, K. I., Pauliny-Toth, I. I. K. & Williams, P. J. S., 1969. *Astrophys. J.*, **157**, 1.
Kühr, H., 1977. *Astr. Astrophys. Suppl.*, **24**, 139.
Kulkarni, V. K., 1978. *Mon. Not. R. astr. Soc.*, **185**, 123.
Longair, M. S. & Scheuer, P. A. G., 1970. *Mon. Not. R. astr. Soc.*, **151**, 45.
McEwan, N. J., Browne, I. W. A. & Crowther, J. H., 1975. *Mem. R. astr. Soc.*, **80**, 1.
Masson, C. R. & Wall, J. V., 1977. *Mon. Not. R. astr. Soc.*, **180**, 193.
Pauliny-Toth, I. I. K., 1977. In *Radio Astronomy and Cosmology (IAU Symp. 74)*, p. 63, ed. Jauncey, D. L., D. Reidel, Dordrecht.
Peacock, J. A. & Wall, J. V., 1981. *Mon. Not. R. astr. Soc.*, **194**, 331.
Peterson, B. A. & Bolton, J. G., 1973. *Astrophys. Lett.*, **13**, 187.
Savage, A., 1978. *PhD Thesis*, University of Sussex.
Schmidt, M., 1972. *Astrophys. J.*, **176**, 273.
Schmidt, M., 1976. *Astrophys. J.*, **209**, L55.
Véron, M. P., Véron, P. & Witzel, A., 1972. *Astr. Astrophys.*, **18**, 82.
Wall, J. V., 1972. *Aust. J. Phys. Astrophys. Suppl.*, **24**, 1.
Wall, J. V., 1980. *Phil. Trans. R. Soc. Lond.*, **A296**, 367.
Wall, J. V. & Cooke, D. J., 1975. *Mon. Not. R. astr. Soc.*, **171**, 9.
Wall, J. V., Pearson, T. J. & Longair, M. S., 1980. *Mon. Not. R. astr. Soc.*, **193**, 683.
Wills, D. & Lynds, R., 1978. *Astrophys. J. Suppl.*, **36**, 317.